Proceedings Paper:
Abdullah, M. and Rossiter, J.A. (2018) The effect of model structure on the noise and disturbance sensitivity of Predictive Functional Control. In: Proceedings of the 2018 European Control Conference (ECC). European Control Conference, 12-15 Jun 2018, Limassol, Cyprus. IEEE, pp. 1009-1014. ISBN: 9781538653036.

https://doi.org/10.23919/ECC.2018.8550374

The effect of model structure on the noise and disturbance sensitivity of Predictive Functional Control

Muhammad Abdullah[1] and John Anthony Rossiter[2]

***Abstract*— An Independent Model (IM) structure has become a standard form used in Predictive Functional Control (PFC) for handling uncertainty. Nevertheless, despite its popularity and efficacy, there is a lack of systematic analysis or academic rigour in the literature to justify this preference. This paper seeks to fill this gap by analysing the effectiveness of different prediction models, specifically the IM structure and T-filter, for handling noise and disturbances. The observations are validated via both closed-loop simulation and real-time implementation and show that the sensitivity relationships are system dependent, which in turn emphasises the importance of performing this analysis to ensure a robust PFC implementation.**

Keywords*—*Predictive Control, PFC, Sensitivity Analysis, Independent model, T-filter, Noise, Disturbance.

I. INTRODUCTION

Predictive Functional Control (PFC) is a variant of Model Predictive Control (MPC) that optimises a cost function solely based on a single degree of freedom (d.o.f) [8], [9]. With this simplification, PFC only requires a minimal computation and indeed, for low order models, the coding is almost trivial. In addition, PFC inherits some benefits of MPC such as systematic handling of constraints and/or systems with delays [10]. Because of its transparent tuning procedure, the controller is widely used in many industrial applications and has become a prime competitor to Proportional Integral Derivative (PID) regulators [4], [9], [10].

Despite its attractive attributes, the simplistic PFC concept is often unable to provide a consistent prediction [11], accurate constrained solutions [1] and effective handling of systems with challenging dynamics [13]. Several works have modified the traditional PFC framework to tackle these weaknesses either via cascade structures [9], pole-placement [13], [14] or input shaping [1]–[3], [13]. However, the derivation of these methods excludes explicit consideration of uncertainty and no attempt was made to discuss or analyse systematically the robustness of PFC.

Generally, PFC has received comparatively little attention in the academic literature because of its weaknesses in providing rigorous properties such as stability assurances [5], [15] or robust feasibility [7]. Critically however, embedding a formal robust design into the PFC formulation conflicts with the requirement for simplicity of coding and implementation [6]; a key selling point of PFC is its simplicity. The normal option is to derive the nominal PFC controller using methods expected to give a robust design [16], [18], such as the use of a T-filter [17] or an Independent Model (IM) [9]. Since the unconstrained PFC framework provides a fixed control law, loop sensitivity can be computed and analysed to assess the controller robustness.

A conventional PFC approach often employs the IM structure to handle uncertainty [9], [10]. However, this paper argues that it is not always the best option to improve sensitivity in general. A user should also consider other alternatives such as the T-filter which may enable better trade-offs between noise and disturbance sensitivity [16], [17]. This paper compares the robustness of these two structures and their sensitivity functions are derived and benchmarked with a nominal PFC based on a CARIMA model. The analysis may help a user to get some insight into how to improve the controller robustness via selecting a suitable PFC structure rather than requiring a more complicated robust design [7].

This paper consists of five main sections. Section II discusses the basic formulation and derivations of sensitivity functions for three different PFC structures: Carima model, T-filter and IM structure. Section III presents the analysis on a real-time example. Section IV analyses two numerical examples with a higher order dynamics and section V provides the concluding remarks.

II. PFC STRUCTURES AND SENSITIVITY FUNCTIONS

This section presents a brief formulation of three different PFC structures associated to different prediction model assumptions together with the derivation of the associated sensitivity functions. Without loss of generality, this paper assumes an underlying CARIMA model (since state space and Finite Impulse Response (FIR) models can equally be represented with a IM). Here, only a brief background on PFC is presented; more detailed derivations, theory and concepts are available in references [4], [9]–[11].

A. PFC with a CARIMA model

The PFC framework is designed based on human intuition where one computes a required control action depending on how fast one desires the output to reach the set point. The first order target trajectory is utilised to define the desired future output by enforcing the equality [11]:

$$y_{k+n|k} = (1-\lambda^n)r + \lambda^n y_k \tag{1}$$

where $y_{k+n|k}$ is the n-step ahead system prediction at sample time k, the desired closed-loop pole λ controls the convergence rate from output y_k to steady-state target r, and

[1,2] M. Abdullah and J.A. Rossiter is with Department of Automatic Control and System Engineering, The University of Sheffield, Mappin Street, S1 3JD, UK. MAbdullah2@sheffield.ac.uk, j.a.rossiter@sheffield.ac.uk@sheffield.ac.uk

[1]M. Abdullah is also with the Department of Mechanical Engineering, International Islamic University Malaysia, Jalan Gombak, 53100, Kuala Lumpur Malaysia. mohd_abdl@iium.edu.my

the coincidence horizon n (a tuning parameter) is when the system prediction is forced to match the target trajectory exactly [9]. Since the n-step ahead prediction algebra for a CARIMA model is well known in the literature (e.g. [16]), only the final form is given here. For input increments Δu_k and outputs y_k, the n-step ahead linear prediction model is:

$$y_{k+n|k} = H\underset{\rightarrow}{\Delta u_k} + P\underset{\leftarrow}{\Delta u_k} + Q\underset{\leftarrow}{y_k} \tag{2}$$

where parameters H, P, Q depend on the model parameters and for a model of order m:

$$\underset{\rightarrow}{\Delta u_k} = \begin{bmatrix} \Delta u_k \\ \Delta u_{k+1} \\ \vdots \\ \Delta u_{k+n-1} \end{bmatrix}; \underset{\leftarrow}{\Delta u_k} = \begin{bmatrix} \Delta u_{k-1} \\ \Delta u_{k-2} \\ \vdots \\ \Delta u_{k-m} \end{bmatrix}; \underset{\leftarrow}{y_k} = \begin{bmatrix} y_k \\ y_{k-1} \\ \vdots \\ y_{k-m} \end{bmatrix} \tag{3}$$

Substituting prediction (2) into equality (1) gives:

$$H\underset{\rightarrow}{\Delta u_k} + P\underset{\leftarrow}{\Delta u_k} + Q\underset{\leftarrow}{y_k} = (1-\lambda^n)r + \lambda^n y_k \tag{4}$$

The constant future input assumption [9], [10] of PFC means $\Delta u_{k+i} = 0$ for $i > 0$, hence only the first column (H_1) of matrix H is used to construct the control law, thus:

$$\Delta u_k = \frac{1}{H_1}\left[(1-\lambda^n)r + \lambda^n y_k - Q\underset{\leftarrow}{y_k} - P\underset{\leftarrow}{\Delta u_k}\right] \tag{5}$$

The control law can be represented in a vector form by rearranging (5) in terms of parameters F, N and $\hat{D}$ with obvious definitions:

$$\Delta u_k = Fr - N\underset{\leftarrow}{y_k} - \hat{D}\underset{\leftarrow}{\Delta u_k} \tag{6}$$

Although the formulation in (6) can be implemented directly, it is easier to utilise a transfer function form for analysing its sensitivity [16]. The vectors of

$$\begin{aligned} N &= [N_0, N_1, N_2, ..., N_n] \\ \hat{D} &= [\hat{D}_0, \hat{D}_1, \hat{D}_2, ..., \hat{D}_n] \end{aligned} \tag{7}$$

are defined in the z domain as:

$$\begin{aligned} N(z) &= N_0 + N_1 z^{-1}, N_2 z^{-2} + ... + N_n z^{-n} \\ \hat{D}(z) &= \hat{D}_0 + \hat{D}_1 z^{-1}, \hat{D}_2 z^{-2} + ... + \hat{D}_n z^{-n} \\ D(z) &= 1 + z^{-1}\hat{D}(z) \end{aligned} \tag{8}$$

Noting the definitions of $\underset{\leftarrow}{\Delta u_k}$ and $\underset{\leftarrow}{y_k}$ in (3), the sensitivity functions are derived based on a fixed closed loop form:

$$D(z)\Delta u_k = F(z)r - N(z)y_k \tag{9}$$

Fig. 1 indicates the equivalent block diagram and adds measurement noise n_k and output disturbance d_k. From the structure, the effective control law can be simplified to $K(z) = N_c(z)[D_c(z)\Delta]^{-1}$. Assuming system $G(z) = B(z)A(z)^{-1}$, the closed-loop pole polynomial $P_c(z) = 1 + K(z)G(z)$ is represented as:

$$P_c(z) = D(z)A(z)\Delta + N(z)B(z) \tag{10}$$

The sensitivity of input to noise is derived by finding the transference from u to n (refer to Fig. 1):

$$\begin{aligned} S_{un} &= K(z)[1 + K(z)G(z)]^{-1} \\ &= N(z)P_c(z)^{-1}A(z) \end{aligned} \tag{11}$$

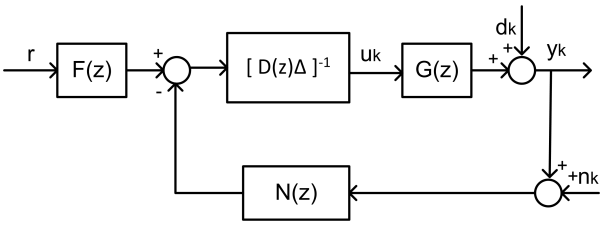

Fig. 1: PFC equivalent block diagram representation.

Similarly, the sensitivity of output to disturbance is obtained by solving the transference from y to d:

$$S_{yd} = [1 + K(z)G(z)]^{-1} = A(z)P_c(z)^{-1}D(z)\Delta \tag{12}$$

Remark 1: This work only considers the sensitivity to noise and output disturbances. Analysis of parameter uncertainty is similar but excluded to save space.

B. PFC with T-Filter (PFCT)

The T-filter acts as a low pass filter to eliminate high frequency measurement noise without affecting the nominal tracking performance [17] of predictive control, although in the literature a T-filter has yet to be applied to PFC. The framework proposed here is a two stage design whereby PFC is first tuned for performance tracking, then the T-filter is employed to improve the sensitivity. Conceptually, the measurement output is low-pass filtered before prediction and anti-filtered after prediction to restore the predicted data back to the correct domain before deploying the nominal algorithm. The procedure is illustrated in Fig. 2 and reduces the impact of high frequency noise on the prediction while retaining the valuable low frequency dynamics [16].

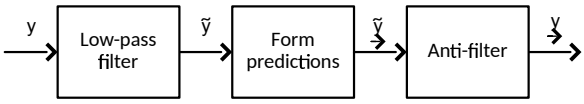

Fig. 2: PFCT prediction structure with T-filter.

The desired T-filter T^{-1} is deployed as $\tilde{y}_k = y_k T^{-1}$ or $T\tilde{y}_k = y_k$. Define the filtered predictions upto horizon n as follows:

$$\underset{\rightarrow}{\tilde{y}}_{k+1} = H\underset{\rightarrow}{\Delta\tilde{u}_k} + P\underset{\leftarrow}{\Delta\tilde{u}_k} + Q\underset{\leftarrow}{\tilde{y}_k} \tag{13}$$

The relationship between the filtered and unfiltered predicted data can be represented using Toeplitz/Hankel form (refer to [16] for more details):

$$\begin{aligned} \underset{\rightarrow}{y}_{k+1} &= C_T\,\underset{\rightarrow}{\tilde{y}}_{k+1} + H_T\underset{\leftarrow}{\tilde{y}_k} \\ \underset{\rightarrow}{\Delta u_k} &= C_T\underset{\rightarrow}{\Delta\tilde{u}_k} + H_T\underset{\leftarrow}{\Delta\tilde{u}_k} \end{aligned} \tag{14}$$

where for $T(z) = T_0 + T_1 z^{-1} + ... + T_n z^{-n}$:

$$C_T = \begin{bmatrix} T_0 & 0 & 0 & \cdots \\ T_1 & T_0 & 0 & \cdots \\ \vdots & \vdots & \vdots & \ddots \\ T_n & T_{n-1} & T_{n-2} & \cdots \end{bmatrix}, H_T = \begin{bmatrix} T_1 & T_2 & \cdots & T_n \\ T_2 & T_3 & \cdots & 0 \\ \vdots & \vdots & \vdots & \ddots \\ 0 & 0 & \cdots & 0 \end{bmatrix} \tag{15}$$

substituting (14) into (13) gives:

$$\underbrace{C_T^{-1}[\underset{\rightarrow}{y}_{k+1} - H_T\underset{\leftarrow}{\tilde{y}_k}]}_{\underset{\rightarrow}{\tilde{y}_k}} = H\underbrace{C_T^{-1}[\underset{\rightarrow}{\Delta u_k} - H_T\underset{\leftarrow}{\Delta\tilde{u}_k}]}_{\underset{\rightarrow}{\Delta\tilde{u}_k}} + P\underset{\leftarrow}{\Delta\tilde{u}_k} + Q\underset{\leftarrow}{\tilde{y}_k} \tag{16}$$

Multiplying through by C_T and grouping common terms:

$$\underset{\rightarrow}{y_k} = H\underset{\rightarrow}{\Delta u_k} + \tilde{P}\underset{\leftarrow}{\Delta\tilde{u}_k} + \tilde{Q}\underset{\leftarrow}{\tilde{y}_k} \tag{17}$$

where $\tilde{P} = [C_T P - HH_T]$ and $\tilde{Q} = [H_T + C_T Q]$. The difference between (17) and (2) are the last two terms which now are based on past filtered data. Hence, applying a similar control law and derivation to eqns.(4-9), a PFCT fixed control law can be formulated as:

$$D_t(z)\Delta u_k = F(z)r - N_t(z)y_k \tag{18}$$

where $D_t(z) = \frac{D(z)}{T(z)}$ and $N_t(z) = \frac{N(z)}{T(z)}$ are represented in the block diagram of Fig. 3. The closed-loop pole polynomial, sensitivity of the input to noise and sensitvity of the output to disturbances are:

$$\begin{aligned} P_t(z) &= D_t(z)A(z)\Delta + N_t(z)B(z) \\ S_{un} &= N_t(z)P_t(z)^{-1}A(z) \\ S_{yd} &= A(z)P_t(z)^{-1}D_t\Delta \end{aligned} \tag{19}$$

Remark 2: It can be shown that the closed-loop poles of PFCT $P_t(z)$ are related to the equivalent poles of PFC by $P_t(z) = P_c(z)T(z)$ and also that the inclusion of T-filter cannot affect the nominal tracking performance [16].

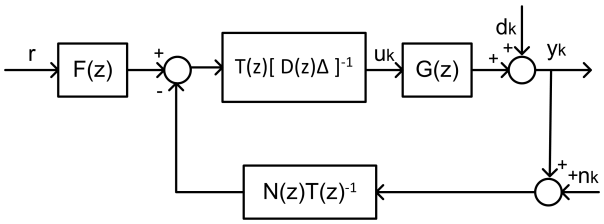

Fig. 3: TPFC fix control loop.

C. PFC with an Independent Model (PFCI)

As discussed before, the IM structure is often used in conventional PFC [9], [10] as the creators believe it gives better sensitivity properties in general. The implementation is equivalent to using a step response model (ignoring truncation errors [16]). Define y_m to be the model output and y_p the process output, then the prediction of future output in (2) is defined based on y_m and augmented with a correction term $D_k = y_{p,k} - y_{m,k}$ as follows:

$$y_{p,k+n|k} = H\underset{\rightarrow}{\Delta u_k} + P\underset{\leftarrow}{\Delta u_k} + Q\underset{\leftarrow}{y_{m,k}} + D_k \tag{20}$$

Equating prediction (20) with the target trajectory (1) gives:

$$H\underset{\rightarrow}{\Delta u_k} + P\underset{\leftarrow}{\Delta u_k} + Q\underset{\leftarrow}{y_{m,k}} - y_{m,k} = (1-\lambda^n)(r - y_{p,k}) \tag{21}$$

Since the future input increment Δu_{k+i} is assumed zero for $i > 0$ and H is reduced to H_1, the PFC control law is:

$$\Delta u_k = \frac{1}{H_1}\left[(1-\lambda^n)r + (1-\lambda^n)y_{p,k} - Q\underset{\leftarrow}{y_{m,k}} + y_{m,k} - P\underset{\leftarrow}{\Delta u_k}\right] \tag{22}$$

For suitable $F, N_i, M_i, \hat{D}$, one can rearrange (22) as:

$$\Delta u_k = Fr - N_i\underset{\leftarrow}{y_{m,k}} - M_i y_{p,k} - \hat{D}\underset{\leftarrow}{\Delta u_k} \tag{23}$$

Transforming (23) into an equivalent transfer function format, the PFCI fixed closed loop is constructed as:

$$D(z)\Delta u_k = F(z)r - N_i(z)y_{m,k} - M_i(z)y_{p,k} \tag{24}$$

The model output can be determined exactly from the model $y_{m,k} = B(z)A(z)^{-1}u_k$ and hence equation (24) can be replaced by (see Fig. 4 for the effective loop structure):

$$\underbrace{[D(z)\Delta + N_i(z)B(z)A(z)^{-1}]}_{D_i(z)}u_k = F(z)r - M_i(z)y_{p,k} \tag{25}$$

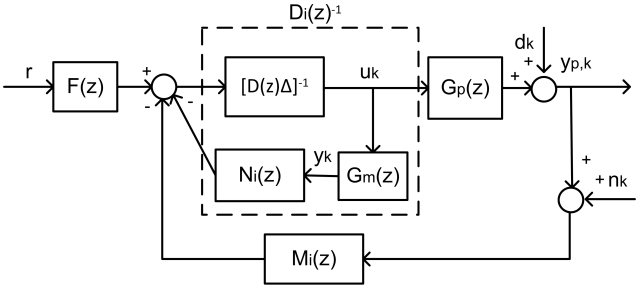

Fig. 4: PFCI fix control loop.

The sensitivities for IM structure of figure 4 are obtained analogously to CARIMA PFC by substituting parameter $D(z)\Delta$ with $D_i(z)$, and $N(z)$ with $M_i(z)$ in equation (10-12). The closed-loop pole polynomial and sensitivites are:

$$\begin{aligned} P_i(z) &= D_i(z)A(z) + M_i(z)B(z) \\ S_{un} &= M_i(z)P_i(z)^{-1}A(z) \\ S_{yd} &= A(z)P_i(z)^{-1}D_i(z) \end{aligned} \tag{26}$$

D. Summary of Control Laws

Table I summarises the sensitivity functions for PFC (Fig. 1), PFCT (Fig. 2) and PFCI (Fig. 4). The key observation is that while, the derivation and structure of all the sensitivity functions are almost same, their parameters are different and hence, different sensitivity response should be expected.

TABLE I: Sensitivity to noise and disturbance.

Algorithm	Input sensitivity to noise	Output sensitivity to disturbance
PFC	$N(z)P_c(z)^{-1}A(z)$	$A(z)P_c(z)^{-1}D(z)\Delta$
PFCT	$N_t(z)P_t(z)^{-1}A(z)$	$A(z)P_t(z)^{-1}D_t(z)\Delta$
PFCI	$M_i(z)P_i(z)^{-1}A(z)$	$A(z)P_i(z)^{-1}D_i(z)$

III. Real Time System Example

This section analyses the sensitivity of a PFC controlled Quanser SRV02 servo based unit [19] system against noise and disturbance. The servo is powered by a Quanser VoltPAQ-X1 amplifier that comes with National Instrument ELVIS II+ multifunctional data acquisition device. The controller is run by National Instrument LabVIEW software via

Fig. 5: Quanser SRV02 servo based unit.

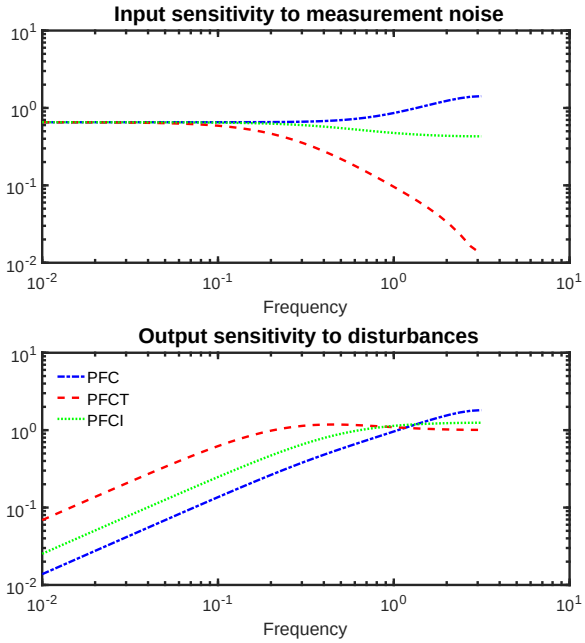

Fig. 6: Sensitivity plot for G_1 with different PFC structures.

USB connection (Fig. 5). The objective is to track the desired servo angular speed, $\dot{\theta}(t)$ by regulating the supplied voltage, $V(t)$. The mathematical model is given as [19]:

$$0.0254\ddot{\theta}(t) = 1.53V(t) - \dot{\theta}(t) \tag{27}$$

where $\ddot{\theta}(t)$ is the servo angular acceleration. Converting the model (27) to discrete form with sampling time $0.02s$, the transfer function of angular speed to voltage input is:

$$G_1 = \frac{0.8338}{1 - 0.455z^{-1}} \tag{28}$$

For a fair comparison, all PFC structures will use the same tuning parameters ($\lambda = 0.7$ and $n = 3$). The sensitivity functions for different loop structures: PFC, PFCT and PFCI are illustrated via Bode plots (see Fig. 6). A summary of observations is given as:

- In the high frequency range, the first order PFCT, $T = 1 - 0.8z^{-1}$ (red dashed line) gives the lowest sensitivity to noise and disturbance followed by PFCI (green dotted line) and PFC (blue dashed-dotted line).
- The output of PFCT is more sensitive to low and mid frequency disturbances compared to PFCI and PFC.

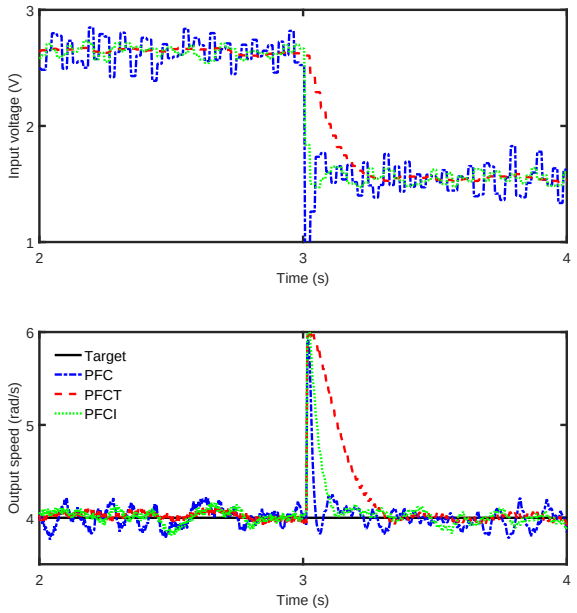

Fig. 7: Closed-loop performance of Quanser servo with different PFC structures.

This observation is then validated by comparing their closed-loop performance on the hardware (see Fig. 7). In this case, the desired angular speed is set at 4 rad/s and the output step disturbance ($d = 2$) entered the system at $3s$. The output measurement is corrupted by Gaussian white noise with amplitude of 2. The results show:

- PFCT reduces noise transmission to the input compared to PFCI and PFC.
- PFCT rejects the output disturbance $0.2s$ slower compared to PFCI and PFC.

In summary, without filter or altered structure, the PFC input is fluctuating between 2.5V to 3V. This situation may lead to a fatigue failure especially for a highly sensitive application. However, improving the sensitivity in one frequency range may make it worst at the other range and hence in practice, a trade-off to get the best overall performance is required. In this example, it may be worth to have a slower disturbance rejection (which is less likely to occur) to get the best noise sensitivity with the T-filter.

IV. Analysis for Higher Order Systems

This section discusses the sensitivity analysis of second order systems with over and under-damped dynamics. The analysis is then validated with their closed-loop performance using Matlab simulations.

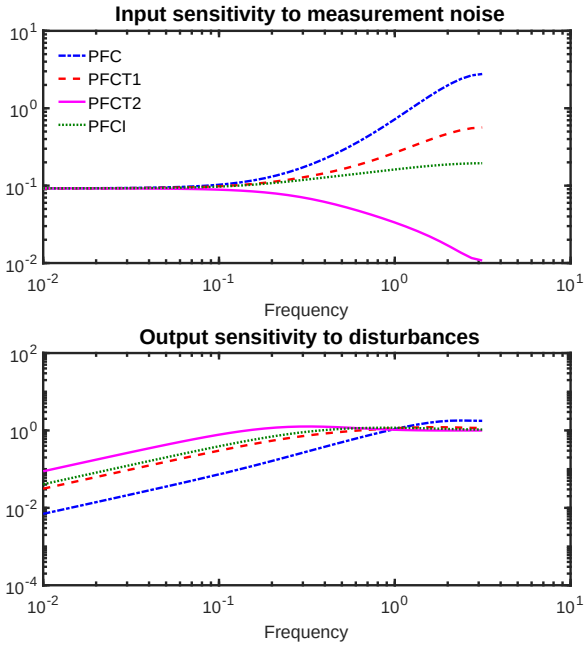

Fig. 8: Sensitivity plot for G_2 with different PFC structures.

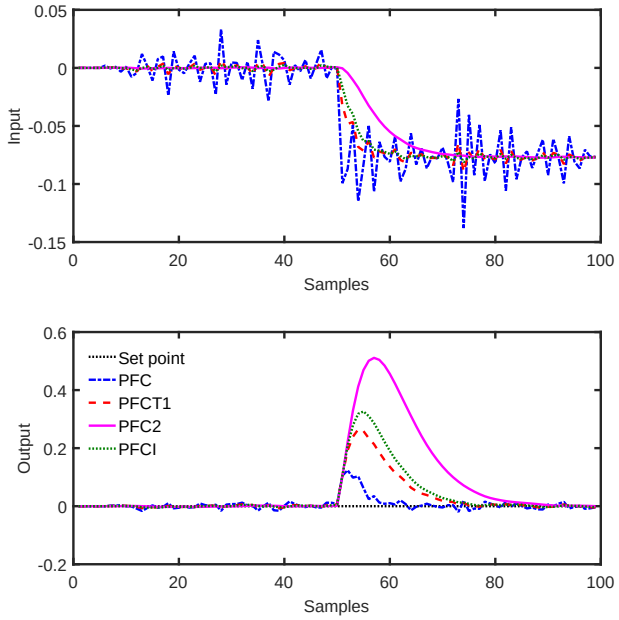

Fig. 9: Closed-loop response of G_2 with corrupted measurement noise and disturbance.

A. Over Damped Second Order System

An over damped second order system (29) is considered here. The set point is zero and a step output disturbance ($d = 0.1$) occurs at the 50th sample. The measurement is corrupted by Gaussian random white noise. All PFCs are tuned with $\lambda = 0.7$ and $n = 3$.

$$G_2 = \frac{z^{-2} + 0.3z^{-1}}{1 - 1.2z^{-1} + 0.32z^{-2}} \tag{29}$$

The Bode plots in Fig. 8 show:

- The input of PFCT2, $T_2 = (1 - 0.8z^{-1})^2$ (pink line) gives the lowest input sensitivity to noise followed by PFCI (green dotted line), PFCT1, $T_1 = 1 - 0.8z^{-1}$ (red dashed line) and PFC (blue dash-dotted line).
- However, over filtering the measurement as with PFCT2 leads to a poor output reaction to disturbances in the low or mid frequency range compared to other structures.

The closed-loop simulation in Fig. 9 reflects the sensitivity analysis whereby:

- PFCT2 rejects most of the noise in input but in fact the variance with PFCI is still small.
- In the present of the output disturbance, PFCT2 converges 7 samples slower than PFCI ($y_{max} = 0.3$) and PFCT1 ($y_{max} = 0.26$) and with the highest overshoot ($y_{max} = 0.5$).

Although, a user can manually tune the T-filter, in this example there is a reasonable argument that the IM structure provides a good sensitivity trade off between noise and disturbances.

B. Second Order Under-damped System

A PFC controlled second order under-damped system (30) again has a zero set point and a disturbance ($d = 0.1$) at 50th sample and measurement noise. The tuning parameter ($\lambda = 0.8$ and $n = 4$) is selected based on the conjecture presented in [2], [11].

$$G_3 = \frac{0.0565z^{-2} + 0.0495z^{-1}}{1 - 1.5643z^{-1} + 0.6703z^{-2}} \tag{30}$$

A similar pattern to the previous example is observed in the Bode diagrams of sensitivity (see Fig. 10):

- PFCT1 gives a small improvement in rejecting high frequency noise, but less than PFCI, while having almost similar disturbance sensitivity in the low frequency range compared to PFCI.
- Over filtering the measurement noise with PFCT2 leads to a more sensitive output to low frequency disturbances.

The closed-loop simulations in Fig. 11 validate the analysis whereby:

- PFCI rejects more noise compared to PFCT1 and almost the same as PFCT2.
- In the presence of the output disturbance, PFCI overshoots more than PFCT1 and less then PFCT2 but converges faster than both.

In this case, it is clearly shown that PFCI has better sensitivity trade-off between noise and disturbances, thus no filter or observer would be recommended.

V. CONCLUSIONS

This work provides a sensitivity analysis to uncertainty for different PFC structures. Although generic conclusions are not applicable, it is clearly shown that the popular IM structure does not always give the best robustness to

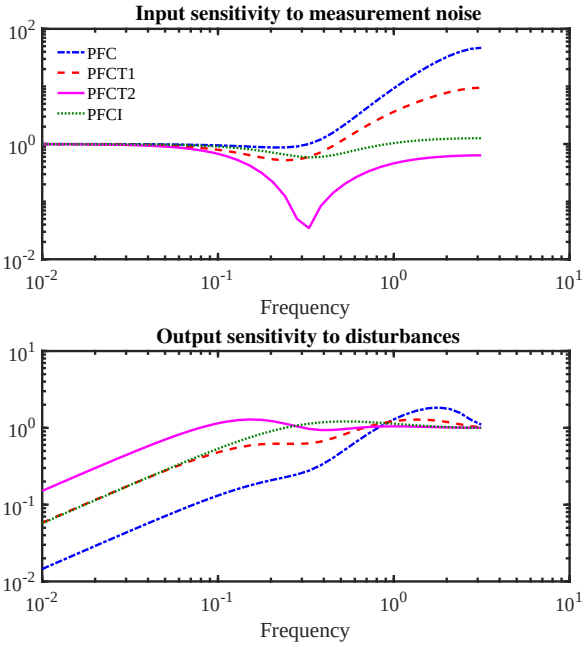

Fig. 10: Sensitivity plot for G_3 with different PFC structures.

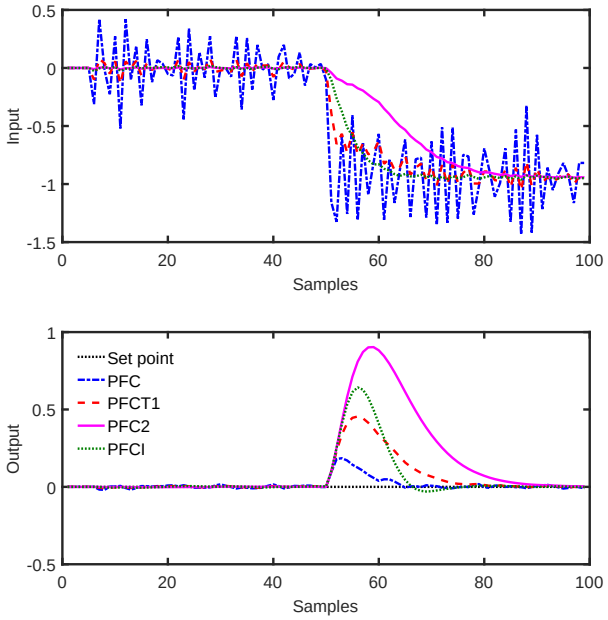

Fig. 11: Closed-loop response for system G_3 with with corrupted measurement noise and disturbance.

uncertainty especially for a simple first order system. In some cases, using a low pass filter such as a T-filter can provide a good sensitivity trade-off between noise and disturbances as shown in the hardware example of section III. However, the sensitivity of PFC structures are system dependent and thus the best option may not be clear a priori as the latter two examples indicated a likely preference for using the IM approach. Hence, production of off-line sensitivity plots is essential to give insight into the robustness of differing PFC structures and indeed, this should be extended to consider a wider range of sensitivity such as parameter uncertainty.

It is also noted that this paper did not consider the impact of changes in the parameters λ, n and one might argue that this should also be investigated. Moreover, where PFC is challenging to tune [12] and/or needs structural changes, further alternative structures may be beneficial and should be included in any offline analysis.

ACKNOWLEDGMENT

The first author would like to acknowledge International Islamic University Malaysia and Ministry of Higher Education Malaysia for funding this work.

REFERENCES

[1] M. Abdullah, J. A. Rossiter and R. Haber, "Development of constrained predictive functional control using laguerre function based prediction," IFAC World Congress, 2017.

[2] M. Abdullah, J. A. Rossiter, "Utilising Laguerre function in predictive functional control to ensure prediction consistency," 11th Int. Conf. on Control, Belfast, UK, 2016.

[3] M. Abdullah, J. A. Rossiter, "Alternative Method for Predictive Functional Control to Handle an Integrating Process", under review for Advances in PID, 2018.

[4] R. Haber, J.A. Rossiter2 and K. Zabet1, "An Alternative for PID control: Predictive Functional Control - A Tutorial," American Control Conference (ACC), 2016, pp. 6935-6940

[5] M. Khadir, J. Ringwood, Stability issues for first order predictive functional controllers: extension to handle higher order internal models, International Conference on Computer Systems and Information Technology (2005) 174-179.

[6] M. Khadir, J. Ringwood, Extension of first order predictive functional controllers to handle higher order internal models, Int. Journal of Applied Mathematics and Comp. Science 18,2, 2008, pp. 229-239.

[7] D. Q. Mayne, M. M. Seron, and S. Rakovic, "Robust model predictive control of constrained linear systems with bounded disturbances, *Automatica*, vol. 41, no. 2, pp. 219224, 2005.

[8] J. Richalet, A. Rault, J.L. Testud and J. Papon, Model predictive heuristic control: applications to industrial processes, Automatica, 14(5), 413-428, 1978.

[9] J. Richalet, and D. O'Donovan, *Predictive Functional Control: principles and industrial applications*. Springer-Verlag, 2009.

[10] J. Richalet, and D. O'Donovan, "Elementary Predictive Functional Control: a tutorial," Int. Symposium on Advanced Control of Industrial Processes, 2011, pp. 306-313.

[11] J. A. Rossiter, and R. Haber, "The effect of coincidence horizon on predictive functional control," *Processes*, 3, 1, pp. 25-45, 2015.

[12] J. A. Rossiter, "Input shaping for PFC: how and why?," *J. Control and Decision*, pp. 1-14, Sep. 2015.

[13] J. A. Rossiter, R. Haber, and K. Zabet, "Pole-placement predictive functional control for over-damped systems with real poles", *ISA Transactions*, vol. 61, pp. 229-239, 2016.

[14] K. Zabet, J. A. Rossiter, R. Haber, and M. Abdullah, "Pole-placement Predictive Functional Control for under-damped systems with real numbers algebra", *ISA Transactions*, In Press., 2017.

[15] J. A. Rossiter, "A priori stability results for pfc, *International journal of control*, vol. 90, no. 2, pp. 305313, 2016.

[16] J. A. Rossiter, *Model predictive control: a practical approach*, CRC Press, 2003.

[17] T.-W. Yoon and D.W. Clarke, Observer design in receding horizon predictive control, International Journal of Control, 61, 171-191, 1995.

[18] K. Zabet and R. Haber, "Robust tuning of PFC (Predictive Functional Control) based on first- and aperiodic second-order plus time delay models", *Journal of Process Control*, vol. 54, pp. 25-37, 2017.

[19] *Quanser user manual SRV02 rotary servo based unit set up and configuration*. Quanser Inc, 2012.